Chapter 5

Light Scattering

Aerosol light scattering plays a major role in the design of aerosol measurement systems (discussed in the next chapter) and radiation transfer through the atmosphere. There are also technological applications in combustion and production of powdered materials. This chapter provides an introduction to the subject.

In broad outline, the problem of light scattering by clouds of small particles can be formulated as follows: Scattering by an individual particle depends on its size, refractive index and shape, and the wavelength of the incident light. There is an extensive literature on the optical properties of single particles (van de Hulst, 1957; Kerker, 1969; Bohren and Huffman, 1983) to which we refer without derivation. The total light scattered from a collimated light beam is obtained by summing the scattering over particles of all sizes and refractive indices, subject to certain limitations discussed in this chapter. In practice, light sources and sinks are distributed in space in a complex way; the radiation intensity at any point is determined by the arrangement of the sources and sinks, the spatial distribution of the aerosol, and its size distribution and composition. In laboratory studies, it is possible to control these variables; and for certain relatively simple configurations (e.g., single scattering and collimated light sources), good agreement can be obtained between theory and experiment. Applications to industrial process gases and to radiation transfer through planetary atmospheres are more complicated. They can sometimes be analyzed using the equation of radiative transfer; an application to atmospheric visibility is discussed.

Central to many applications is the integration of an optical parameter, such as the total or angular scattering, over the particle size distribution. The optical thickness (turbidity) of an aerosol is an important case. Several examples are discussed for different forms of the size distribution functions. In the inverse problem not discussed in this text, the particle size distribution can sometimes be estimated from scattering measurements (Bayvel and Jones, 1981). Most of the phenomena discussed in this chapter involve elastic light scattering in which the frequency of the scattered light is equal to that of the incident beam. At the end of the chapter, we discuss examples in which the frequency of the scattered light is different from that of the incident beam, including quasi-elastic light scattering and inelastic scattering (the Raman effect). Quasi-elastic light scattering refers to weak displacements of the frequency of the scattered beam from the incident wavelength. Applications are to the measurement of the size of very small particles. Raman scattering is potentially important

for on-line measurement of aerosol chemical components. A summary diagram based on simple quantum mechanical concepts illustrates various scattering processes.

SCATTERING BY SINGLE PARTICLES: GENERAL CONSIDERATIONS

When aerosol particles interact with light, two different types of processes can occur. The energy received can be reradiated by the particle in the same wavelength. The reradiation may take place in all directions but usually with different intensities in different directions. This process is called *scattering*. Alternatively, the radiant energy can be transformed into other forms of energy, such as (a) heat and (b) energy of chemical reaction. This process is called *absorption*. In the visible range, light attenuation by absorption predominates for black smokes, whereas scattering controls for water droplets. The next few sections focus on elastic scattering and absorption.

It is convenient to analyze the light attenuation process by considering a single particle of arbitrary size and shape, irradiated by a plane electromagnetic wave (Fig. 5.1). The effect of the disturbance produced by the particle is to diminish the amplitude of the plane wave. At a distance large compared with the particle diameter and the wavelength, the scattered energy appears as a spherical wave, centered on the particle and possessing a phase different from the incident beam. The total energy lost by the plane wave, the extinction energy, is equal to the scattered energy in the spherical wave plus the energy of absorption.

In many applications, the most important characteristic of the scattered wave is its intensity, I, expressed in cgs units as erg/cm^2 sec. At large distances from the origin, the energy flowing through a spherical surface element is $Ir^2 \sin\theta \, d\theta \, d\phi$. This energy flows radially and depends on θ and ϕ but not on r. It is proportional to the intensity of the incident beam I_0 and can be expressed as follows:

$$Ir^2 \sin\,\theta \, d\theta \, d\phi = I_0 \left(\frac{\lambda}{2\pi}\right)^2 F(\theta,\ \phi,\ \lambda) \sin\,\theta \, d\theta \, d\phi \tag{5.1}$$

or

$$I = \frac{I_0 F(\theta,\ \phi,\ \lambda)}{(2\pi r/\lambda)^2} \tag{5.2}$$

The wavelength of the incident beam, λ, is introduced in the denominator to make the scattering function, $F(\theta,\ \phi,\ \lambda)$, dimensionless. In general, $F(\theta,\ \phi,\ \lambda)$ depends on the wavelength of the incident beam and on the size, shape, and optical properties of the particles but not on r. For spherical particles, there is no ϕ dependence. The relative values of F can be plotted in a polar diagram as a function of θ for a plane in the direction of the incident beam. A plot of this type is called the *scattering diagram* for the particle.

The scattering function can be determined from theory for certain important special cases as discussed in the following sections. The performance of optical single-particle counters (Chapter 6) depends on the variation of the scattering function with angular position, and much effort has been devoted to the design of such detectors.

The intensity function, by itself, is not sufficient to characterize the scattered light. Needed also are the polarization and phase of the scattered light, which are discussed in the

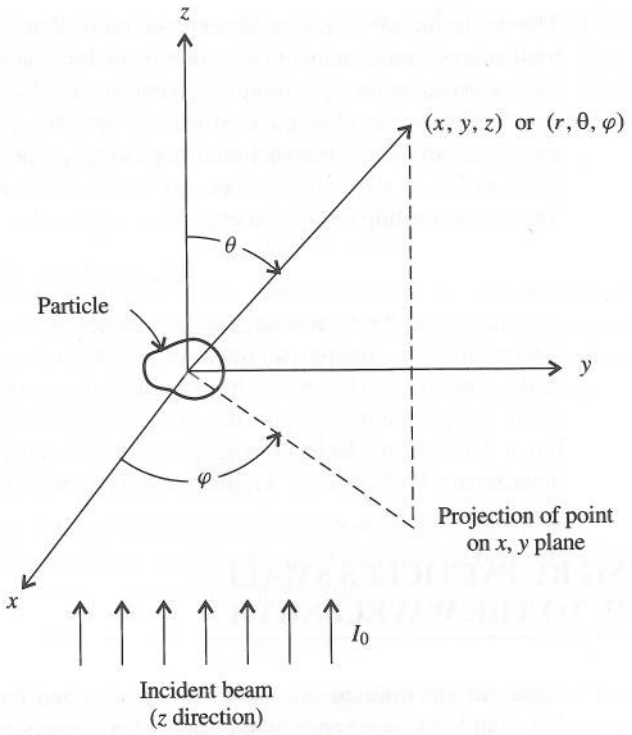

Fig. 5.1 The direction of scattering at any r is characterized by the scattering angle, θ, measured relative to the direction of the incident beam, and the azimuth angle, ϕ.

standard references on the subject. For many applications including atmospheric scattering and optical instrument design, the parameters of most interest are the intensity function and related quantities, defined as follows: Let the total energy scattered in all directions by the particle be equal to the energy of the incident beam falling on the area C_{sca}:

$$C_{\text{sca}} = \frac{1}{I_0}\int_0^{2\pi}\int_0^{\pi} Ir^2 \sin\,\theta\, d\theta\, d\phi$$

$$= \frac{1}{(2\pi/\lambda)^2}\int_0^{2\pi}\int_0^{\pi} F(\theta,\ \phi,\ \lambda)\sin\,\theta\, d\theta\, d\phi \tag{5.3}$$

This defines the *scattering cross section* C_{sca}, which has the dimension of area but is not in general equal to the particle cross-sectional area. Indeed it is customary to define the *scattering efficiency*

$$Q_{\text{sca}} = C_{\text{csa}}/s_g \tag{5.4}$$

where s_g is the geometric cross section. Combining (5.3) and (5.4), we obtain

$$Q_{\text{sca}} = \frac{\int_0^{2\pi}\int_0^{\pi} F(\theta,\ \phi,\ \lambda)\, d\theta\, d\phi}{(2\pi/\lambda)^2 s_g} \tag{5.5}$$

The scattering efficiency represents the ratio of the energy scattered by the particle to the total energy in the incident beam intercepted by the geometric cross section of the particle. As discussed below, Q_{sca} may be greater than unity.

Similarly, the absorption efficiency is defined as the fraction of the incident beam absorbed per unit cross-sectional area of particle. The total energy removed from the incident beam, the extinction energy, is the sum of the energy scattered and absorbed. The corresponding extinction efficiency is given by

$$Q_{ext} = Q_{sca} + Q_{abs} \tag{5.6}$$

In the next three sections, the dependence of the scattering efficiency on particle size is discussed; in the first two sections, very small and very large particles are considered. Both of these ranges can be treated from a relatively simple point of view. However, many light-scattering problems fall into the more complex intermediate size range discussed later. For a detailed, readable monograph on light scattering by single particles, stressing the determination of $F(\theta, \phi, \lambda)$, the reader is referred to van de Hulst (1957).

SCATTERING BY PARTICLES SMALL COMPARED TO THE WAVELENGTH

Light, an electromagnetic wave, is characterized by electric and magnetic field vectors. For simplicity, we consider the case of a plane wave, linearly polarized, incident on a small spherical particle. The wavelength of light in the visible range is about 0.5 μm. For particles much smaller than the wavelength, the local electric field produced by the wave is approximately uniform at any instant. This applied electric field induces a dipole in the particle. Because the electric field oscillates, the induced dipole oscillates; and according to classical theory, the dipole radiates in all directions. This type of scattering is called *Rayleigh scattering*.

The dipole moment, $\mathbf{p}$, induced in the particle is proportional to the instantaneous electric field vector:

$$\mathbf{p} = \alpha \mathbf{E} \tag{5.7}$$

This expression defines the polarizability, α, which has the dimensions of a volume and which is a scalar for an isotropic spherical particle. From the energy of the electric field produced by the oscillating dipole, an expression can be derived for the intensity of the scattered radiation:

$$I = \frac{(1 + \cos^2 \theta) k^4 \alpha^2}{2r^2} I_0 \tag{5.8}$$

where the wave number $k = 2\pi/\lambda$. The scattering is symmetrical with respect to the direction of the incident beam with equal maxima in the forward and backward directions and the minimum at right angles (Fig. 5.4 for $x < 0.6$).

Because the intensity of the scattered light varies inversely with the fourth power of the wavelength, blue light (short wavelength) is scattered preferentially to red. This strong dependence leads to the blue of the sky (in the absence of aerosol particles) and

contributes to the red of the sunset when the red-enriched transmitted light is observed. In polluted atmospheres, however, molecular scattering is usually small compared with aerosol scattering. The principal contribution to scattering comes from a larger particle size range in which the Rayleigh theory does not apply. This is discussed in a later section.

For an isotropic spherical particle, it can be shown that

$$\alpha = \frac{3\left(m^2-1\right)}{4\pi\left(m^2+2\right)}v \tag{5.9}$$

where m is the refractive index of the particle and v is the volume, $\pi d_p^3/6$. This result is valid regardless of the shape of the scatterer so long as the particle is much smaller than the wavelength of the light. When scattering without absorption takes place, the efficiency factor is obtained by substituting (5.9) and (5.8) in (5.5) and integrating:

$$Q_{\text{sca}} = \frac{8}{3}x^4\left\{\frac{m^2-1}{m^2+2}\right\}^2 \tag{5.10}$$

where $x = \pi d_p/\lambda$ is the dimensionless optical particle size parameter.

Both scattering and absorption can be taken into account by writing the refractive index as the sum of a real and an imaginary component:

$$m = n - in' \tag{5.11}$$

where $n^2+n'^2 = \epsilon$ and $nn' = \lambda\sigma/c$, where ϵ is the dielectric constant, σ is the conductivity, λ is the wavelength in vacuum, and c is the velocity of light. The imaginary term gives rise to absorption; it vanishes for nonconducting particles ($\sigma = 0$). Both ϵ and σ depend on λ, approaching their static values at low frequencies. For metals in the optical frequency range, both n and n' are of order unity. The scattering efficiency of small spherical absorbing particles is given by (van de Hulst, 1957)

$$Q_{\text{sca}} = \frac{8}{3}x^4\text{Re}\left\{\frac{m^2-1}{m^2+2}\right\}^2 \tag{5.12}$$

where Re indicates that the real part of the expression is taken. The absorption efficiency is

$$Q_{\text{abs}} = -4x\text{Im}\left\{\frac{m^2-1}{m^2+2}\right\} \tag{5.13}$$

where Im indicates that the imaginary part is taken. For very small particles of absorbing material, the particle extinction coefficient varies only with the first power of x and the total extinction per particle obtained by multiplying Q_{abs} by the cross section is proportional to the particle volume.

For scattering alone, an expansion of the efficiency factor in x based on Mie theory discussed below gives

$$Q_{\text{ext}} = \frac{8}{3}x^4\left(\frac{m^2-1}{m^2+2}\right)^2\left[1+\frac{6\left(m^2-1\right)}{5\left(m^2+2\right)}x^2+\ldots\right] \tag{5.14}$$

When $m = 1.5$ corresponding to certain organic liquids and many metallic salts, the second term in the second bracket is less than 0.1 for $x < 0.53$. Thus the Rayleigh form can be

used with an error of less than 10% for green light ($\lambda = 0.5\ \mu$m) when $d_p < 0.084\ \mu$m and $m = 1.5$.

SCATTERING BY LARGE PARTICLES: THE EXTINCTION PARADOX

For particles much larger than the wavelength of the incident light ($x \gg 1$), the scattering efficiency approaches 2. That is, a large particle removes from the beam *twice* the amount of light intercepted by its geometric cross-sectional area. What is the explanation for this paradox?

For light interacting with a large particle, the incident beam can be considered to consist of a set of separate light rays. Of those rays passing within an area defined by the geometric cross section of the sphere, some will be reflected at the particle surface and others refracted. The refracted rays may emerge, possibly after several internal reflections. Any of the incident beam that does not emerge is lost by absorption within the particle. Hence all of the energy incident on the particle surface is removed from the beam by scattering or absorption, accounting for an efficiency factor of unity.

There is, however, another source of scattering from the incident beam. The portion of the beam not intercepted by the sphere forms a plane wave front from which a region corresponding to the cross-sectional area of the sphere is missing. This is equivalent to the effect produced by a circular obstacle placed normal to the beam. The result, according to classical optical principles, is a diffraction pattern *within the shadow area* at large distances from the obstacle. The appearance of light within the shadow area is the reason why diffraction is sometimes likened to the bending of light rays around an obstacle.

The intensity distribution within the diffraction pattern depends on the shape of the perimeter and size of the particle relative to the wavelength of the light. It is independent of the composition, refractive index, or reflective nature of the surface. The total amount of energy that appears in the diffraction pattern is equal to the energy in the beam intercepted by the geometric cross section of the particle. Hence the total efficiency factor based on the cross-sectional area is equal to 2.

The use of the factor 2 for the efficiency requires that all scattered light be counted including that at small angles to the direction of the beam. In general, the observation must be made at a large distance from the particle compared with the particle size. As van de Hulst points out, a flower pot in a window blocks only the sunlight falling on it, and not twice that amount, from entering a room; a meteorite of the same size in space between a star and a telescope on Earth will remove twice the amount of starlight falling on it. Because the distance of the detector from a scattering aerosol particle is large compared with the particle diameter, $Q_{sca} \rightarrow 2.0$ for $x \gg 1$.

SCATTERING IN THE INTERMEDIATE SIZE RANGE: MIE THEORY

General Considerations

Rayleigh scattering for $x \ll 1$ and the large particle extinction law for $x \gg 1$ provide useful limiting relationships for the efficiency factor. Frequently the range $x \sim 1$ is important.

Atmospheric visibility, for example, is limited by particles whose size is of the same order as the wavelength of light in the optical range, from 0.1 to 1 μm in diameter (McCartney, 1976). In this range, the theory of Rayleigh is no longer applicable because the field is not uniform over the entire particle volume. Such particles are still too small for large particle scattering theory to be applicable. As a result, it is necessary to make use of a much more complicated theory due to Mie, which treats the general problem of scattering and absorption of a plane wave by a homogeneous sphere. Expressions for the scattering and extinction are obtained by solving Maxwell's equations for the regions inside and outside the sphere with suitable boundary conditions. It is found that the efficiency factors are functions of x and m alone. This represents a general scaling relationship for light scattering by isotropic spheres. Scattering efficiency calculations must be carried out numerically, and the results for many cases have been tabulated. The theory, sources of detailed calculations and their interpretation are discussed by van de Hulst (1957) and Kerker (1969). Useful computer programs are given by Barber and Hill (1990).

For water, $m = 1.33$, whereas for organic liquids it is often approximately 1.5. The scattering efficiency for these two values of m are shown in Fig. 5.2 as a function of the dimensionless particle diameter x. For $x \to 0$, the theory of Rayleigh is applicable.

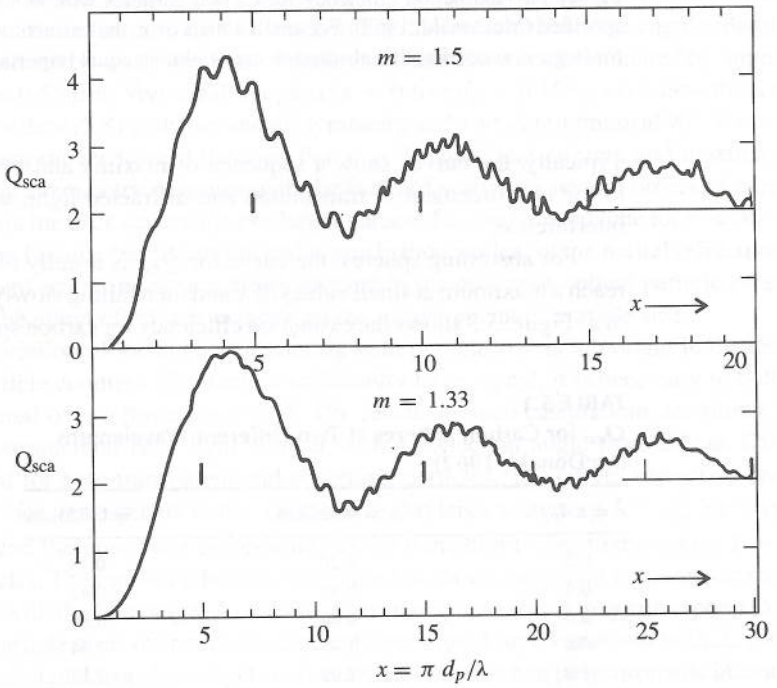

Figure 5.2 Extinction curves calculated from the theory of Mie for $m = 1.5$ and $m = 1.33$ (van de Hulst, 1957). The curves show a sequence of maxima and minima of diminishing amplitude, typical of nonabsorbing spheres with $1 < m < 2$. Indeed, by taking the abscissa of the curve for $m = 1.5$ to be $2x(m - 1)$, all extinction curves for the range $1 < m < 2$ are reduced to approximately the same curve.

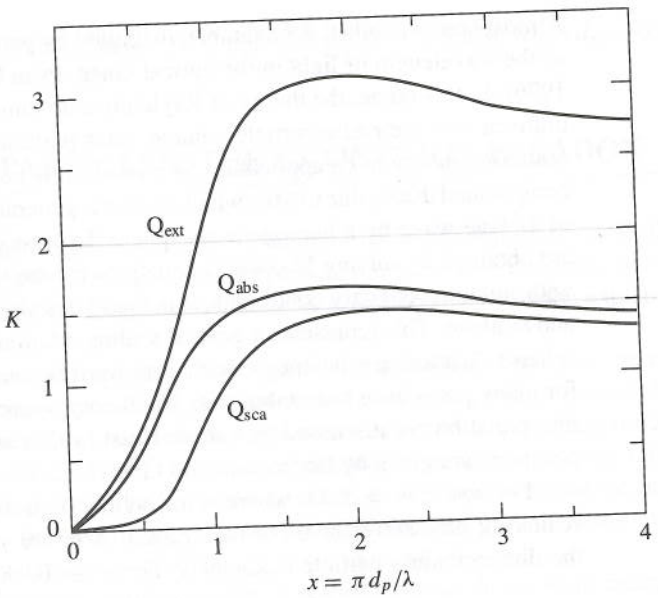

Figure 5.3 Extinction efficiency for carbon particles with $m = 2.00(1 - 0.33i)$, temperature not specified (McDonald, 1962). For small values of x, the extinction is due primarily to absorption; but for large x, scattering and absorption are of almost equal importance.

Typically, the curves show a sequence of maxima and minima: The maxima correspond to the reinforcement of transmitted and diffracted light, while the minima correspond to interference.

For absorbing spheres, the curve for Q_{ext} is usually of simpler form, rising rapidly to reach a maximum at small values of x and then falling slowly to approach two at large values of x. Figure 5.3 shows the extinction efficiency for carbon spheres. For such particles, nearly

TABLE 5.1
Q_{ext} for Carbon Spheres at Two Different Wavelengths (McDonald, 1962)

$x = \pi d_p/\lambda$	$\lambda = 0.436\mu m$	$\lambda = 0.623\mu m$
0.2	0.20	0.18
0.4	0.46	0.42
0.6	0.86	0.82
0.8	1.45	1.44
1.0	2.09	2.17
1.5	2.82	2.94
2.0	3.00	3.09
4.0	2.68	2.68
8.0	2.46	2.46

all of the scattering is due to diffraction, while almost all of the geometrically incident light is absorbed. The refractive index for absorbing spheres usually varies with wavelength, and this results in the variation of Q_{ext} as well. As shown in Table 5.1, however, the variation over the visible spectrum is not great.

Angular Scattering

Mie scattering by single particles irradiated by conventional laser sources is sufficiently strong to be detected at high signal-to-noise ratios for particles larger than about 0.1 μm. The noise results from Rayleigh scattering by the gas molecules and from the instrument electronics. The signal depends in a complex way on the angle of the detector with respect to the scattering particle, as well as on the particle size and refractive index.

The angular dependence of the light scattering can be calculated from Mie theory. For values of x approaching unity and small values of $m (< 2.0)$, an asymmetry favoring forward scattering appears. For very large values of m corresponding to opaque or reflecting particles, there is an asymmetry toward back scattering. For $x \gg 1$, forward scattering increases still more strongly (Fig. 5.4), showing very rapid changes for small increases in the scattering angle θ. The scattered light in the $x \gg 1$ limit can be considered to consist of three components interpreted according to classical theory as diffraction, reflection, and refraction.

Some of these features are illustrated in Fig. 5.4, which shows the angular distribution of light scattered by water droplets of different diameters when illuminated by unpolarized light of $\lambda = 0.55$ μm. Very small droplets ($x < 0.6$ or $d_p < 0.106$ μm) follow the Rayleigh scattering pattern (5.8) with fore and aft symmetry and a weak minimum at 90°. For $x > 0.6$, the minimum moves toward the rear. For $x > 3$, additional minima and maxima appear and a strong asymmetry develops with the forward scattering several orders of magnitude stronger than the back scattering. For larger values of x, the forward lobe for $\theta < 30°$ results mainly from Fraunhofer diffraction and is nearly independent of the partial refractive index. Thus forward scattering is sometimes favored in the design of optical particle counters to eliminate the effect of refractive index on the measurement of particle size.

The variation of the angular scattering with particle size is important in the design of optical particle counters. To obtain a sufficiently large signal, it is necessary to collect the light scattered over a finite range of θ. The results of such calculations are shown in Fig. 5.5 for a commercial laser light counter with a collection angle from 35° to 120° from the forward for both transparent and absorbing particles. The curves show two branches: The lower one corresponds to the approach to Rayleigh scattering $I \sim d_p^6$ for very small particles, and the upper one corresponds to the transition to geometric optics $I \sim d_p^2$ for large particles. The transition between the branches shows the strong variations in scattering associated with the Mie range. As a result, a given response signal may correspond to several different particle sizes over certain ranges of operation. Large variations with d_p present in the scattered signal from laser light sources are smoothed when polychromatic incandescent sources with multiple wavelengths are used as shown in Chapter 6.

Scattering cross sections have been measured for liquid suspensions of transparent, irregular particles graded in size by sedimentation (Hodkinson, 1966). The shapes of the curves of the scattering cross sections were simpler than those of spherical particles, but

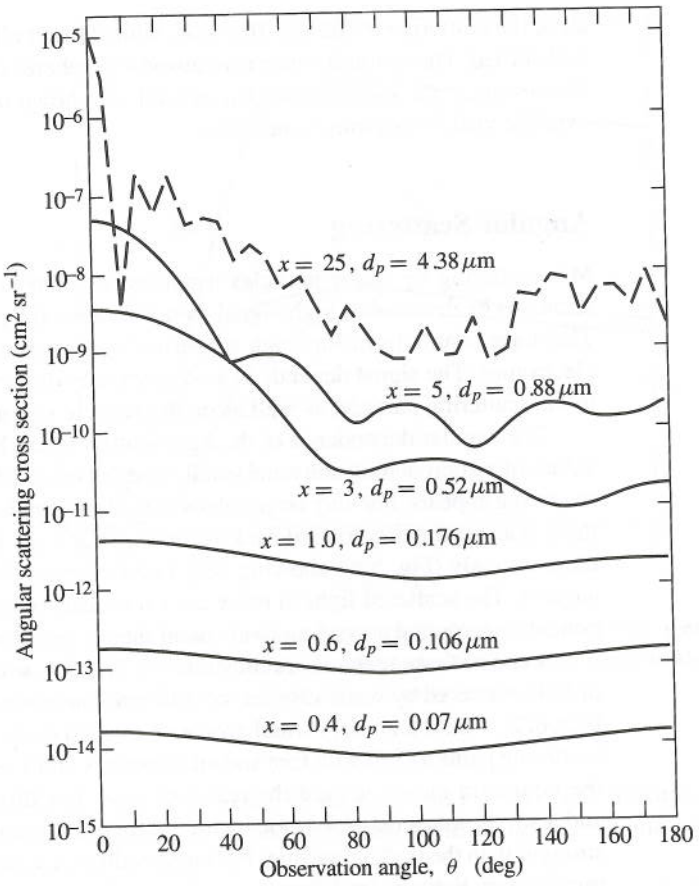

Figure 5.4 Angular scattering for water droplets illuminated by unpolarized light. The results hold for light in the visible range; the indicated values of d_p correspond to $\lambda = 0.55\ \mu$m (after McCartney, 1976). Very small droplets ($x < 0.6$) show the Rayleigh scattering pattern (5.8) with fore and aft symmetry and a weak minimum at right angles. Larger particles display strong variations with θ associated with scattering in the Mie range.

theoretical predictions have not been made except for very small particles to which the Rayleigh theory is applicable.

SCATTERING BY AEROSOL CLOUDS

General Considerations

We consider the case of an aerosol illuminated by a collimated light source of a given wavelength. The experimental arrangement is shown schematically in Fig. 5.6. A photometer of this type installed in a smoke stack or duct would be suitable for measuring the attenuation

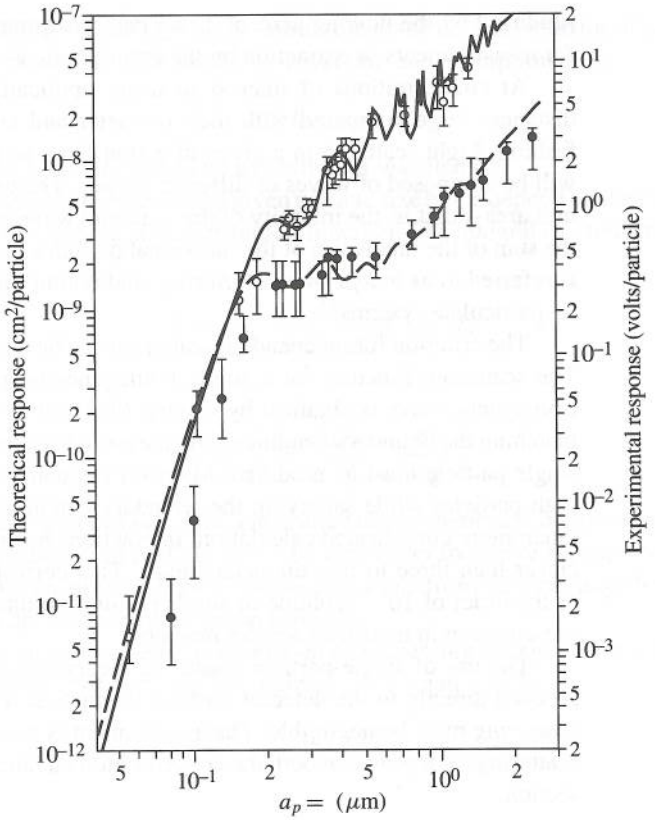

Figure 5.5 Variation of light scattering over the angle from 35° to 120° from the forward direction for a He–Ne laser light source ($\lambda = 0.633$ μm). Particles were latex ($m = 1.588$) and nigrosin dye ($m = 1.67 - 0.26i$). The lower branch shows the approach to the Rayleigh scattering range (response $\sim d_p^6$), and the upper branch shows the approach to geometric optics (response $\sim d_p^2$) (Garvey and Pinnick, 1983).

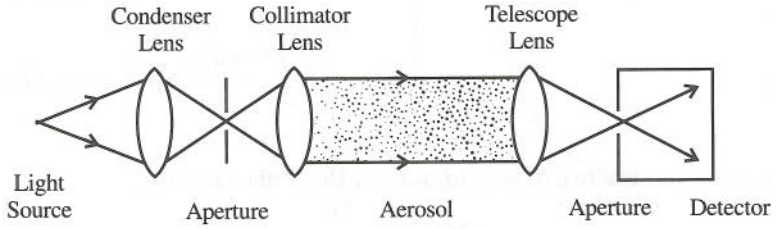

Figure 5.6 Schematic diagram of an apparatus for the measurement of the extinction produced by a cloud of small particles. The goal is to measure only transmitted light and not light scattered by the particles. In practice, light of decreased intensity from the source is measured together with a certain amount of light scattered at small angles from the forward direction by the particles. (After Hodkinson, 1966.)

produced by the flowing aerosol. Long path instruments of this kind have also been used for measurements of extinction by the atmospheric aerosol.

At concentrations of interest in many applications, the particles are separated by distances large compared with their diameter and are distributed in space in a random fashion. Light scattered in a given direction from an incident beam by different particles will be composed of waves of different phases. The total energy of the scattered wave per unit area—that is, the intensity of the scattered wave in a given direction—will be equal to the sum of the intensities of the individual particles in that direction. This type of behavior is referred to as *independent scattering*, and it simplifies calculation of the total scattering by particulate systems.

The criterion for independent scattering can be clarified by referring to the last section. The scattering function for a single homogeneous sphere interacting with a plane electromagnetic wave is obtained by solving Maxwell's equations for the gas and sphere and matching the boundary conditions. As the particles approach each other, the solution for the single particle must be modified. Maxwell's equations must be solved inside and outside both particles while satisfying the boundary conditions at the particle surfaces. This is a much more complicated calculation. Interactions become important when the particles are closer than three to five diameters apart. This corresponds to volumetric concentrations of the order of 10^{-2} (volume of solids per unit volume of gas), much higher than usually present even in industrial aerosol reactors.

The use of single-particle scattering theory also requires that the scattered radiation proceed directly to the detector without interaction with other particles. That is, *multiple scattering* must be negligible. This requirement is more stringent than that of independent scattering; it depends on both the concentration and the path length as discussed in the next section.

Extinction Coefficient and Optical Thickness

If there are dN particles in the size range d_p to $d_p + d(d_p)$ per unit volume of air, this corresponds to a total particle cross-sectional area of $(\pi d_p^2/4)dNdz$ over the light path length, dz, per unit area normal to the beam. The attenuation of light over this length is given by the relation

$$-dI = I\left[\int_0^\infty \frac{\pi d_p^2}{4} Q_{\text{ext}}(x,\ m) n_d(d_p) d(d_p)\right] dz \tag{5.15}$$

where $dN = n_d(d_p)d(d_p)$. Hence the quantity

$$b = -\frac{dI}{I\,dz} = \int_0^\infty \frac{\pi d_p^2}{4} Q_{\text{ext}}(x,\ m) n_d(d_p) d(d_p) \tag{5.16}$$

represents the fraction of the incident light scattered and absorbed by the particle cloud per unit length of path. It is called the *extinction coefficient* (sometimes the *attenuation*

coefficient or *turbidity*), and it plays a central role in the optical behavior of aerosol clouds. In terms of the separate contributions for scattering and absorption (5.6),

$$b = b_{sca} + b_{abs} \tag{5.17}$$

where each term is understood to be a function of wavelength.

The contributions to $b(\lambda)$ from a given particle size range depend on the extinction cross section and on the particle size distribution function. The integral (5.16) can be rearranged as follows:

$$b = \int_{-\infty}^{\infty} \frac{db}{d \log d_p} d \log d_p \tag{5.18}$$

where

$$\frac{db}{d \log d_p} = \frac{3}{2} \frac{Q_{ext}}{d_p} \frac{dV}{d \log d_p} \tag{4.18a}$$

This function has been evaluated for a measured atmospheric size distribution and is shown in Fig. 5.7 as a function of particle size. The area under the curve is proportional to b. The figure shows that the principal contributions to b come from the size range between 0.1 and 3 μm. This occurs frequently for urban aerosols.

The reduction in the intensity of the light beam passing through the aerosol is obtained by integrating (5.16) between any two points, $z = L_1$ and $z = L_2$:

$$I_2 = I_1 e^{-\tau} \tag{5.19}$$

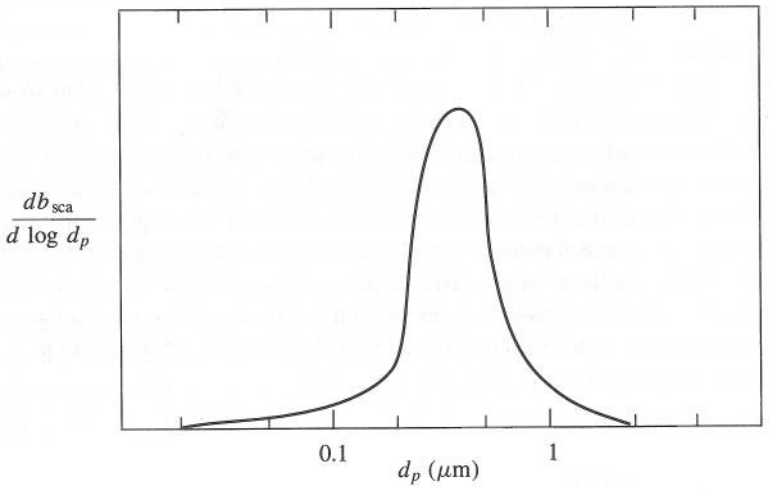

Figure 5.7 Contributions to the scattering coefficient as a function of particle size for the Pasadena, CA, aerosol (August 1969) based on the calculations of Ensor et al. (1972). The curve was calculated from the measured particle size distribution assuming $m = 1.5$. Largest contributions to light scattering came from the 0.2- to 0.5-μm size range for calculations made over the wavelength range 0.365 μm $< \lambda <$ 0.675 μm.

where the optical thickness, $\tau = \int_{L_1}^{L_2} b\, dz$, is a dimensionless quantity; b has been kept under the integral sign to show that it can vary with position, as a result of spatial variation in the aerosol concentration. Equation (5.19) is a form of Lambert's law. Limitations on the use of (5.19) resulting from multiple scattering are usually stated in terms of τ (van de Hulst, 1957). For $\tau < 0.1$ the assumption of single scattering is acceptable, while for $0.1 < \tau < 0.3$ it may be necessary to correct for double scattering. For $\tau > 0.3$, multiple scattering must be taken into account. The problem of multiple scattering for Rayleigh gases was solved by Chandrasekhar (1960). For particles in the Mie range, approximate methods for the calculation of multiparticle scattering are available (Bayvel and Jones, 1981). For a polluted urban region where aerosol scattering dominates, the value of b_{sca} is of the order of 10^{-3} m^{-1}. Taking $\tau < 0.1$ as the criterion for single scattering, the maximum distance for the passage of a beam in which single scattering dominates is $0.1(10)^3$ or 100 m.

SCATTERING OVER THE VISIBLE WAVELENGTH RANGE: AEROSOL CONTRIBUTIONS BY VOLUME

In many cases of practical interest, the incident light—solar radiation for example—is distributed with respect to wavelength. The contribution to the integrated intensity I from the wavelength range λ to $\lambda + d\lambda$ is

$$dI = I_\lambda\, d\lambda \tag{5.20}$$

where I_λ is the intensity distribution function. The loss in intensity over the visible range, taking into account only single scattering, is determined by integrating (5.20) over the wavelength:

$$d\left(\int_{\lambda_1}^{\lambda_2} I_\lambda\, d\lambda\right) = -\left[\int_{\lambda_1}^{\lambda_2} b(\lambda) I_\lambda\, d\lambda\right] dz \tag{5.21}$$

where λ_1 and λ_2 refer to the lower and upper ranges of the visible spectrum and b is now regarded as a function of λ. We wish to determine the intensity loss resulting from the particulate volume present in each size range of the size distribution function. For constant aerosol density, this is equivalent to the mass in each size range. Knowing the contributions of the various chemical components to the mass in each size range, a quantitative link can be made between the extinction and the components of the aerosol, as discussed in Chapter 13.

Substituting (5.18) and (5.19) in (5.21), the result is

$$\bar{b} = \int_{\lambda_1}^{\lambda_2} b(\lambda) f(\lambda)\, d\lambda = \int_{-\infty}^{\infty} G(d_p) \frac{dV}{d \log d_p} d \log d_p \tag{5.22}$$

where

$$G(d_p) = \frac{3}{2d_p} \int_{\lambda_1}^{\lambda_2} Q_{ext}(x, m) f(\lambda)\, d\lambda \tag{5.22a}$$

$f(\lambda)\, d\lambda$ is the fraction of the incident radiation in the range λ to $\lambda + d\lambda$, and $f(\lambda)$ has been normalized with respect to the total intensity in the range between λ_1 and λ_2. The quantity

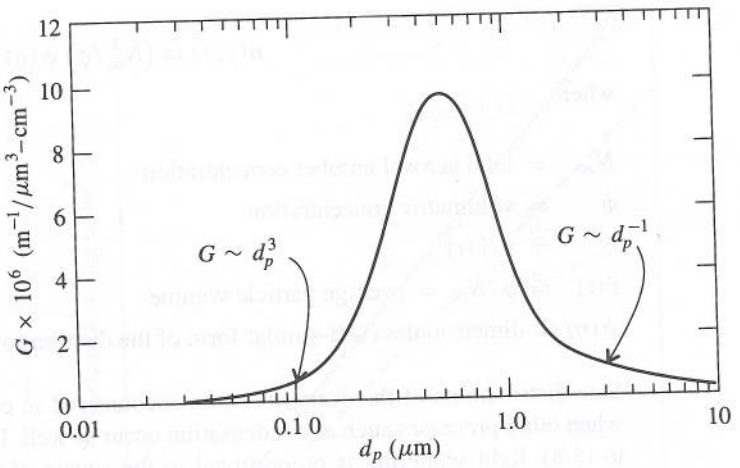

Figure 5.8 Light scattering per unit volume of aerosol material as a function of particle size, integrated over all wavelengths for a refractive index, $m = 1.5$. The incident radiation is assumed to have the standard distribution of solar radiation at sea level (Bolz and Tuve 1970). The limits of integration on wavelength were 0.36 to 0.680 μm. The limits of visible light are approximately 0.350 to 0.700 μm. The curve is independent of the particle size distribution.

$G(d_p)$ represents the extinction over all wavelengths between λ_1 and λ_2 per unit volume of aerosol in the size range between d_p and $d_p + d(d_p)$. It is independent of the particle size distribution function. For a refractive index, $m = 1.5$, $G(d_p)$ has been evaluated for the standard distribution of solar radiation at sea level, using Mie scattering functions. The result is shown in Fig. 5.8 as a function of particle size.

A number of interesting features are exhibited by this curve: The oscillations of the Mie functions (Fig. 5.3) are no longer present because of the integration over wavelength. For $d_p \to 0$ in the Rayleigh scattering range, $G(d_p) \sim d_p^3$. For large d_p, $G(d_p)$ vanishes because Q_{sca} approaches a constant value (two) at all wavelengths; as a result, $G(d_p) \sim d_p^{-1}$ for $d_p \to \infty$. The most efficient size for light scattering on a mass basis corresponds to the peak in this function, which, for $m = 1.5$, occurs in the size range between 0.5 and 0.6 μm. Particles of 0.1-μm diameter, on the one hand, and 3 μm on the other contribute only one-tenth the scattering on an equal mass basis. The volume distribution $dV/d \log d_p$ of atmospheric aerosols often shows a peak in the 0.1- to 3-μm size range. This reinforces the importance of this range to total light scattering. In the next two sections, examples are given of calculations of total scattering by two different type of aerosol size distribution functions.

RAYLEIGH SCATTERING: SELF-SIMILAR SIZE DISTRIBUTIONS

An important class of self-similar particle size distributions $n(v, t)$ can be represented by an equation of the form (Chapters 1 and 7):

$$n(v,t) = \left(N_\infty^2/\phi\right)\psi(\eta) \tag{5.23}$$

where

N_∞ = total aerosol number concentration
ϕ = volumetric concentration
η = $v/\bar{v}(t)$
$\bar{v}(t)$ = ϕ/N_∞ = average particle volume
$\psi(\eta)$ = dimensionless self-similar form of the distribution function

Size distributions of this form are often encountered in coagulating aerosols, sometimes when other processes such as condensation occur as well. In the Rayleigh range, according to (5.8), light scattering is proportional to the square of the particle volume; when two particles of the same size combine to form a larger one, the total light scattered doubles. This is true so long as the two original particles are separated by a distance much greater than the wavelength of the incident light. In this case, the two particles scatter independently and out of phase, and the energy of the scattered light is the sum of the energies scattered separately by the two particles. When the two particles are combined and still much smaller than the wavelength of the light, the electric field scattered will be the sum of the two electric fields in phase. As a result, double the amplitude of the single particle or four times the energy of a single particle will be scattered. Hence the light scattered by a coagulating small particle aerosol increases with time.

For self-similar particle size distributions, the average particle size can be determined directly by measuring the extinction. Total scattering in the Rayleigh range is

$$b_{sca} = B\int_0^\infty n(v)v^2\,dv \tag{5.24}$$

where

$$B = \frac{24\pi^3}{\lambda^4}\left|\frac{m^2-1}{m^2+2}\right|^2$$

Substituting the self-similar form for the size distribution function, (5.23), we obtain

$$b_{sca} = B\phi\bar{v}\int_0^\infty \psi(\eta)\eta^2\,d\eta \tag{5.24a}$$

The integral in (5.24a) is a constant that depends on the form of the size distribution function. For the special case of coagulating, coalescing aerosols composed of spherical particles, the integral is 2.01 (Chapter 7) and

$$b_{sca} = 2.01B\phi\bar{v} \tag{5.25}$$

Hence for a coagulating aerosol with constant ϕ, the scattered light intensity is proportional to the instantaneous mean particle volume, $\bar{v} = \phi/N$. Thus by measuring the extinction, the average particle volume $\bar{v}$ can be determined for this special case. No arbitrary constants appear in the analysis.

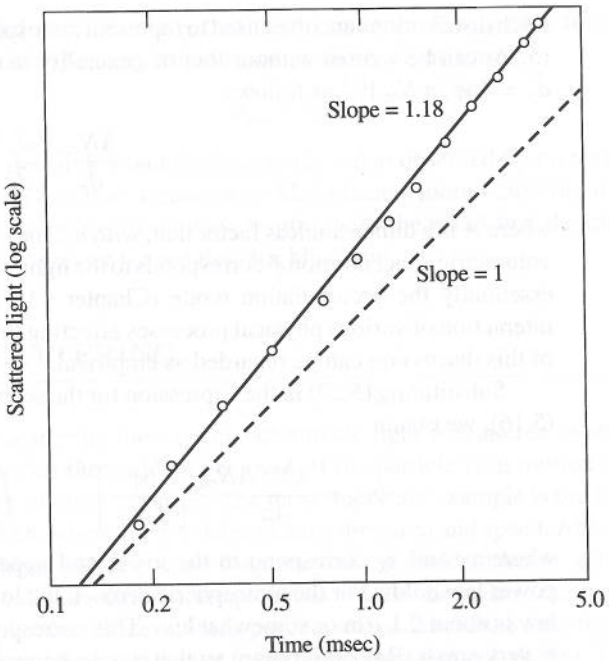

Figure 5.9 Increase, with time, of light scattered by coagulating lead particles generated by the decomposition of tetramethyl lead. The light source was an argon laser (Graham and Homer, 1973). As coagulation takes place, the total light scattering increases although N_∞ decreases and ϕ stays constant. This figure applies to free molecule aerosols.

Light scattering by a coagulating aerosol in the Rayleigh size range was measured by Graham and Homer (1973). The aerosol was generated by passing a shock wave through argon containing tetramethyl lead (TML). The TML decomposes behind the shock to form a supersaturated lead vapor that nucleates and produces small lead droplets that subsequently coagulate. The rate of coagulation was followed by measuring light scattered perpendicular to the incident argon laser beam (Fig. 5.9). The slope in logarithmic coordinates is very close to the theoretical value of 6/5 (Chapter 7).

If there are many particles larger than the Rayleigh range, calculations based on (5.25) underestimate particle size. The measured scattering by the larger particles will generally be less than the value calculated, assuming that the particles were in the Rayleigh range.

MIE SCATTERING: POWER LAW DISTRIBUTIONS

Aerosol size distributions can sometimes be represented by a power law relationship in the size subrange $0.1 < d_p < 3\ \mu$m, where most of the contribution to light scattering occurs:

$$n_d(d_p) \sim d_p^{-p} \tag{5.26}$$

Such distributions are often used to represent atmospheric and clean room aerosols. Equation (5.26) can be written without loss of generality in terms of the average particle diameter $\bar{d}_p = [6\phi/\pi N_\infty]^{1/3}$ as follows:

$$n_d = \frac{AN_\infty}{\bar{d}_p}\left(\frac{d_p}{\bar{d}_p}\right)^{-p} \tag{5.27}$$

where A is a dimensionless factor that, with $\bar{d}_p$, may be a function of time and position. The volumetric concentration ϕ corresponds to the light-scattering subrange ($0.1 < d_p < 3$ μm), essentially the accumulation mode (Chapter 13). Equation (5.27) may result from the interaction of various physical processes affecting the size distribution, but for the purposes of this discussion can be regarded as empirical.

Substituting (5.27) in the expression for the scattering part of the extinction coefficient, (5.16), we obtain

$$b_{\text{sca}} = \frac{\lambda^{3-p}AN_\infty}{4\pi^{2-p}}\left[\frac{6\phi}{\pi N_\infty}\right]^{(p-1)/3}\int_{x_1}^{x_2} Q_{\text{sca}}(x,m)x^{2-p}\,dx \tag{5.28}$$

where x_1 and x_2 correspond to the lower and upper limits, respectively, over which the power law holds. For the atmospheric aerosol, the lower limit of applicability of the power law is about 0.1 μm or somewhat less. This corresponds to $x_1 < 1$, and for this range Q_{sca} is very small (Rayleigh range) so that x_1 can be replaced by zero. The contribution to the integral for large values of x is also small because p is usually greater than 3 or 4 and Q_{sca} approaches a constant, 2. Hence the upper limit x_2 can be set equal to infinity as a good approximation. The result is

$$\begin{aligned} b_{\text{sca}} &= \frac{\lambda^{3-p}AN_\infty}{4\pi^{2-p}}\left[\frac{6\phi}{\pi N_\infty}\right]^{(p-1)/3}\int_0^\infty Q_{\text{sca}}(x,m)x^{2-p}\,dx \\ &= AA_1\lambda^{3-p}N_\infty^{(4-p)/3}\phi^{(p-1)/3} \end{aligned} \tag{5.29}$$

where A_1 is a constant defined by this expression. Thus if the distribution obeys a power law (5.26) and (5.27), the order, p, can be determined by measuring the wavelength dependence of the extinction coefficient. Moreover, for the power law distribution, the wavelength dependence of b_{sca} is independent of the shape of the extinction curve, provided that it satisfies the asymptotic limiting relationships discussed above.

Experimentally, it is sometimes found that

$$b_{\text{sca}} = A_2\phi \tag{5.30}$$

where A_2 is a constant. This corresponds to $p = 4$ and constant A; by (5.27) we obtain

$$n_d = \frac{6A\phi}{\pi d_p^4} \tag{5.31}$$

a power law form that often holds approximately for the light-scattering subrange of the atmospheric aerosol. However, (5.31) cannot extend to infinitely large particle diameters because the aerosol volumetric concentration becomes logarithmically infinite. Equation (5.30) holds better when the value of ϕ corresponds to the subrange $0.1 < d_p < 1$ μm rather than the total volumetric concentration. The constants, of course, differ.

It is also found experimentally that the dependence of b_{sca} on λ for the atmospheric aerosol can sometimes be represented by an equation of the form

$$b_{sca} \sim \lambda^{-1.3} \tag{5.32}$$

corresponding to $p = 4.3$, which is close to the value observed by direct measurement of the size distribution function. Equation (5.32) indicates more scattering in the blue (short wavelength) than in the red (long wavelength), with the result that the range of vision in hazy atmospheres is greater for red than for blue light.

QUASI-ELASTIC LIGHT SCATTERING

In classical light-scattering theory, monochromatic light is scattered in all directions with the same frequency as the incident beam ω_0. If the particle is in motion with respect to a fixed observer, the situation changes. The most important example is the Brownian motion (Chapter 2) in which submicron particles change direction and speed. Although the moving particle scatters light with the same frequency as the incident beam, a fixed observer or detector will see a slightly different frequency $\omega = \omega_0 + \Delta\omega$, where the frequency shift $\Delta\omega$ is an optical Doppler shift. If the emitting particle moves toward the detector, the light it emits appears more blue-shifted; if it moves away it appears more red-shifted. The Doppler shift depends only on the particle velocity and not on its material or optical properties. Particles of a given size have a Maxwellian velocity distribution determined by the equipartition principle and the absolute temperature (Chapter 2).

The Doppler shift is very small compared with the main frequency. To a close approximation, it is given by

$$\Delta\omega = \frac{v}{c}\omega_0 \tag{5.33}$$

where v is the particle velocity with respect to the detector and c is the velocity of light. Because the mean thermal speed of a 0.1-μm particle is of the order of 10 cm/sec, it is clear that the Doppler shift is very small. For this reason it can be neglected in the classical light-scattering studies discussed above. However, with suitable instrumentation, it is possible to detect the shift averaged over the particles and determine the particle size in this way. The phenomenon is called *quasi-elastic light scattering* (QELS); the frequency shift is so small that the scattering is nearly elastic (Berne and Pecora, 1976; Dahneke, 1983). QELS, also known as photon correlation spectroscopy or dynamic light scattering, can be used to measure the size of monodisperse particles in the size range from 0.01 to a few tenths of a micron. The method is widely used for small particles and large molecules suspended in aqueous solutions. It has also been applied in a few cases to aerosols (Dahneke, 1983).

In a QELS system, a laser beam is passed through a cloud of Brownian particles. Light is scattered into the detector that is set at an angle θ with respect to the incident beam. The scattering volume is defined by the intersection between the incident and the detector collection solid angles. The instantaneous intensity of the scattered light along a given path $I(t)$ can be written as the sum of the average intensity, $\bar{I}$, and a fluctuating intensity, $I'(t)$

$$I(t) = \bar{I} + I'(t) \tag{5.34}$$

The time-averaged scattered intensity $\bar{I}$ is the basis of conventional light-scattering techniques used for aerosol measurements.

The intensity fluctuations due to the Brownian motion take place on a time scale much faster than conventional photometers or the human eye can detect. The variation in the fluctuating scattered light intensity with time resembles a noise signal that can be analyzed in terms of its correlation function with respect to time. The usual practice is to measure the polarized intensity time correlation function that is related to the diffusion coefficient for monodisperse particles as follows

$$G(\xi) = \overline{I(t)I(t+\xi)} = A\left[1 + \beta|\alpha^2 N_\infty g(\xi)|^2\right] \tag{5.35}$$

where

A = baseline constant
β = instrument constant
α = molar polarizability of the particles
$g(\xi)$ = normalized autocorrelation function for the translational Brownian motion
N_∞ = average particle concentration

For monodisperse particles

$$g(\xi) = \exp\left(-q^2 \xi D\right) \tag{5.36}$$

where D = particle diffusion coefficient and $q = (4\pi/\lambda)\sin(\theta/2)$. The autocorrelation function $g(\xi)$ is the parameter sought, and from it the diffusion coefficient, hence particle diameter can be obtained. The procedures have been worked out in most detail for application to hydrosols and high-molecular-weight polymeric solutions (Dahneke, 1983).

Rearranging (5.35) gives the autocorrelation function in terms of the experimentally measured variable $G(\xi)$:

$$\alpha^2 N_\infty g(\xi) = \frac{1}{\sqrt{A\beta}}\left[G(\xi) - A\right]^{1/2} \tag{5.37}$$

Various methods are used to determine the diffusion coefficient. For example after subtraction of the baseline constant, A, $G(\xi)$ may be fitted to an exponential function to permit calculation of the decay constant $q^2 D$, hence particle size from the value of D.

For polydisperse aerosols, the simple expression (5.36) for the autocorrelation function must be averaged over the particle size distribution function. In the Rayleigh scattering range

$$N_\infty g(\xi) = \int_0^\infty n_d(d_p) d_p^6 \exp\left(-q^2 \xi D\right) d(d_p) \tag{5.38}$$

There is no general exact method for extracting size distribution functions $n_d(d_p)$ from (5.38) and the experimentally measured function $G(\xi)$ when the form of $n_d(d_p)$ is not known. In the method of cumulants, the one most commonly used to estimate hydrosol size distributions from this integral, the logarithm of the autocorrelation function $g(\xi)$ is expanded in ξ:

$$\ln\, g(\xi) = K_1 \xi - K_2 \frac{\xi^2}{2} + \ldots \tag{5.39}$$

The coefficients of ξ are moments of the size distribution function known as *cumulants*. In practice, only the first two cumulants can be accurately determined from the experimental data:

$$K_1 = q^2 \bar{D} \tag{5.40a}$$

and

$$K_2 = q^4 \overline{(D - \bar{D})^2} \tag{5.40b}$$

Here the averaging is weighted by d_p^6 as in (5.38). For a free molecule aerosol we have $D \sim d_p^{-2}$ (Chapter 2), so $\bar{D}$ is proportional to the fourth moment of the particle size distribution. This heavily weights the upper end of the distribution function. If the form of the distribution function is known, the cumulants can be used to evaluate the parameters of the distribution. For example, if the size distribution is self-preserving (Chapter 7), any moment can be used to estimate the complete distribution.

SPECIFIC INTENSITY: EQUATION OF RADIATIVE TRANSFER

In the general case of aerosol/light interactions in the atmosphere or within a confined space, the light is neither unidirectional nor monochromatic; each volume element is penetrated in all directions by radiation. This requires a more careful definition of the intensity of radiation than used before. For the analysis of this case, an arbitrarily oriented small area, $d\sigma$, is chosen with a normal $\mathbf{n}$ (Fig. 5.10). At an angle θ to the normal we draw a line S, the axis of an elementary cone of solid angle $d\omega$. If through every point of the boundary of the area $d\sigma$ a line is drawn parallel to the nearest generator of the cone $d\omega$, the result is a truncated semi-infinite cone $d\Omega$, similar to the cone $d\omega$. Its cross-sectional area, perpendicular to S at the point P, will be $d\sigma \cos\theta$.

Let dE be the total quantity of energy passing in time dt through the area $d\sigma$ inside cone $d\Omega$ in the wavelength interval λ to $\lambda + d\lambda$. For small $d\sigma$ and $d\omega$, the energy passing through $d\sigma$ inside $d\Omega$ will be proportional to $d\sigma\, d\omega$.

The specific intensity of radiation or simply the intensity, I_λ, is defined by the relation

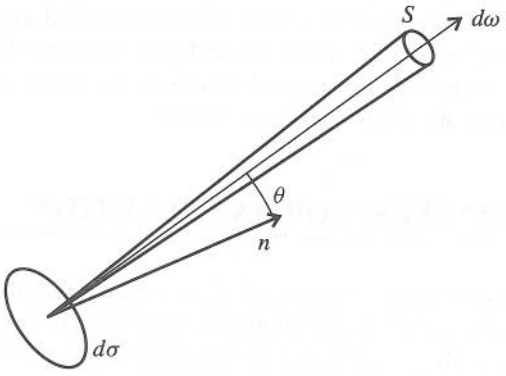

Figure 5.10 Geometric factors determining specific intensity of radiation.

$$I_\lambda = \frac{dE}{d\sigma \cos\theta \, dt \, d\omega \, d\lambda} \tag{5.41}$$

The intensity is, in general, a function of the position in space of the point P, the direction $\mathbf{s}$, time t, and wavelength λ:

$$I_\lambda = I_\lambda(P, \mathbf{s}, t, \lambda) \tag{5.42}$$

If I_λ is not a function of direction, the intensity field is said to be *isotropic*. If I_λ is not a function of position the field is said to be *homogeneous*. The total intensity of radiation is $I = \int_0^\infty I_\lambda \, d\lambda$. In the rest of this chapter, we suppress the suffix λ to simplify the notation.

Now consider the radiant energy traversing the length, ds, along the direction in which the intensity is defined; a change in the intensity results from the combination of the effects of extinction (absorption and scattering) and emission:

$$dI(P, s) = dI(\text{extinction}) + dI(\text{emission}) \tag{5.43}$$

The loss by extinction can be written as before in terms of the extinction coefficient, b:

$$dI(\text{extinction}) = -bI \, ds \tag{5.44}$$

Emission by excited dissociated atoms and molecules in the air is usually small in the visible compared with solar radiation. Thermal radiation is important in the far infrared but not in the visible. Hence consistent with the assumptions adopted in this chapter, gaseous emissions can be neglected in the usual air pollution applications.

In an aerosol, however, a *virtual emission* exists because of rescattering in the s direction of radiation scattered from the surrounding volumes. The gain by emission is written in the form of a source term:

$$dI(\text{emission}) = bJ \, ds \tag{5.45}$$

This equation defines the source function, J.

Hence the energy balance over the path length, ds, takes the form

$$-\frac{dI}{b \, ds} = I - J \tag{5.46}$$

which is the *equation of radiative transfer*. This equation is useful, as it stands, in defining atmospheric visibility as discussed in a later section. Detailed applications require an expression for the source function, J, which can be derived in terms of the optical properties of the particles, but this is beyond the scope of this book. For further discussion, the reader is referred to Chandrasekhar (1960) and Goody (1964).

EQUATION OF RADIATIVE TRANSFER: FORMAL SOLUTION

The equation of radiative transfer is an energy balance; except for this concept, its physical content is slight. The physical problems of interest enter through the extinction coefficient and the source function. Many papers and monographs have been written on its solution

for different boundary conditions and spatial variations of the optical path (Chandrasekhar, 1960; Goody, 1964). Some simple solutions are discussed in this and the next section. Most of the applications have been to planetary atmospheres and astrophysical problems rather than to configurations of industrial interest or small scale pollution problems.

The formal solution of the equation of transfer is obtained by integration along a given path from the point $s = 0$ (Fig. 5.11):

$$I(s) = I(0)e^{-\tau(s,\,0)} + \int_0^s J(s')e^{-\tau(s,\,s')}b\,ds' \tag{5.47}$$

where $\tau(s,\ s')$ is the optical thickness of the medium between the points s and s':

$$\tau(s, s') = \int_{s'}^{s} b\,ds \tag{5.48}$$

The source function $J(s')$ over the interval 0 to s must be known to evaluate the integral in (5.47).

The interpretation of (5.47) is interesting: The intensity at s is equal to the sum of two terms. The first term on the right-hand side corresponds to Lambert's law (5.19), often used for the attenuation of a light beam by a scattering medium. The second term represents the contributions to the intensity at s from each intervening radiating element between 0 and s, attenuated according to the optical thickness correction factor. In the absence of external light sources and if secondary scattering by the surrounding aerosol can be neglected, the source function J becomes zero. This is the situation for configuration of a properly designed transmissometer, which is used to measure the attenuation of a light beam through the smoke flowing through a stack and in other industrial applications.

When the medium extends to $-\infty$ in the s direction and there are no sources along s, it may be convenient not to stop the integration at the point 0 but to continue it indefinitely:

$$I(s) = \int_{-\infty}^{s} J(s')e^{-\tau(s,\,s')}b\,ds' \tag{5.49}$$

Thus the intensity observed at s is the result of scattering by all of the particles along the line of sight.

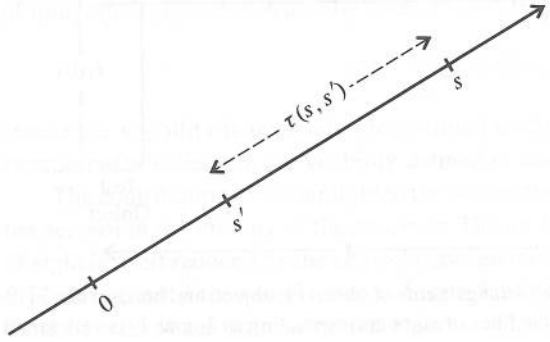

Figure 5.11 Path of integration along the s vector. Light at point 0 reaches any point s attenuated according to Lambert's law. In addition, light is scattered toward s by particles between 0 and s such as those at the point s'.

LIGHT TRANSMISSION THROUGH THE ATMOSPHERE: VISIBILITY

An important and interesting application of the theory of radiative transfer is to the definition of atmospheric visibility. The terms "visibility" and "visual range" may be used interchangeably to signify the distance at which it is just possible to distinguish a dark object against the horizon. As pointed out by Middleton (1952), "the problem, then, is to establish usable theoretical relationships between light, eye, target, and atmosphere that will permit the calculation of the visual range at any time; and to provide means of measuring the necessary parameters quickly and accurately enough." This can be accomplished by solving the equation of radiative transfer, subject to a set of assumptions concerning human response to the obscuration of objects.

Most of the information that we obtain through our sense of vision depends on our perception of differences in intensity or of color among the various parts of the field of view. An object is recognized because its color or brightness differs from its surroundings, and also because of the variations of brightness or color over its surface. The shapes of objects are recognized by the observation of such variations.

Differences in intensity are particularly important and are the principal basis for the classical theory of visibility (Steffens, 1956): An isolated object on the ground such as a building is viewed from a distance along a horizontal line of sight (Fig. 5.12). The intensity contrast between the test object and the adjacent horizon sky is defined by the expression

$$C = \frac{I_1 - I_2}{I_2} \tag{5.50}$$

where I_2 is the intensity of the background and I_1 is the intensity of the test object, both measured at the same distance from the observer.

Expressions for the intensity can be obtained by integrating the equation of radiative transfer (5.46) over the horizontal distance from the test object to the point of observation. If b and J are not functions of s, the integration gives

$$I(s) = I(0)e^{-bs} + J\left[1 - e^{-bs}\right] \tag{5.51}$$

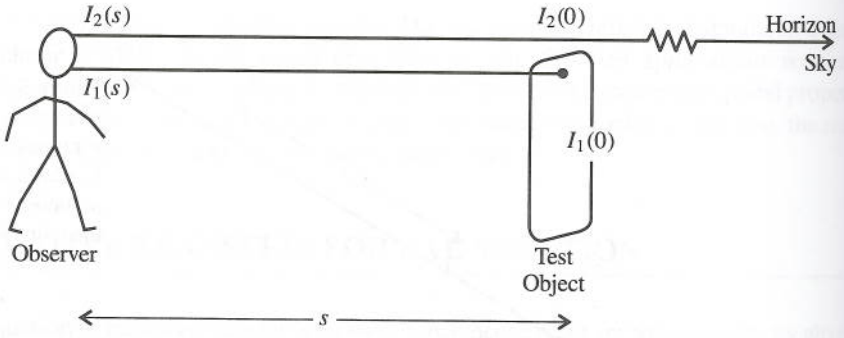

Figure 5.12 Relative arrangements of observer, object, and horizon sky in definition of the visibility. The angle between the lines of sight corresponding to I_1 and I_2 is very small.

where $s = 0$ corresponds to the location of the test object. Rewriting (5.50) as

$$C = \frac{I_2(0)}{I_2(s)} \frac{[I_1(s) - I_2(s)]}{I_2(0)} \tag{5.52}$$

and substituting (5.51) for $[I_1(s) - I_2(s)]$ gives with (5.50)

$$C = \frac{I_2(0)}{I_2(s)} \frac{[I_1(0) - I_2(0)]\, e^{-bs}}{I_2(0)} = \frac{I_2(0)}{I_2(s)} C(0) e^{-bs} \tag{5.53}$$

where $C(0)$ is the contrast at the test object.

In viewing the horizon sky, the observer sees the virtual emission, J, resulting from the light from the sun and surroundings scattered in the direction of the observer by the atmosphere. This is sometimes referred to as the air light or the skylight. By assumption, the air light is not a function of s. Suppose that 2 refers to the line of sight in the direction of the horizon sky. The intensity at any plane normal to this sightline is equal to the virtual emission or air light J; that is, $I_2(s) = I_2(0) = J =$ constant and (5.53) becomes

$$C = C(0) e^{-bs} \tag{5.54}$$

If the test object is perfectly black, then $I_1(0) = 0$, $C(0) = -1$, and

$$C = -e^{-bs} \tag{5.55}$$

The minus sign in this expression results because the test object is darker than the background.

The visual range or, more commonly, the visibility is defined as the distance at which the test object is just distinguishable from background. Hence the minimum contrast that the eye can distinguish must now be introduced into the analysis. This contrast is denoted by C^* and the corresponding visibility $s = s^*$. For a black object at $s = s^*$,

$$C^* = -\exp(-bs^*) \tag{5.56}$$

or

$$s^* = -\frac{1}{b} \ln(-C^*) \tag{5.57}$$

The parameter C^* is sometimes called the threshold contrast or "psychophysical constant" because it depends on human perception. Based on data averaged over responses of a group of individuals, its value is usually taken to be 0.02:

$$s^* = -\frac{1}{b} \ln\, 0.02 = \frac{3.912}{b} \tag{5.58}$$

Hence the visibility is inversely proportional to the extinction coefficient. Because b is a function of wavelength, the visibility defined in this way also depends on wavelength.

The contribution of the air light to the obscuration of distant objects comes mostly from the aerosol in the vicinity of the observer. The air light from more distant parts of the line of sight is itself reduced by the aerosol between its region of origin and the observer. Figure 5.13 shows that if the visual range is 1 mile, half of the obscuration would be produced by the 0.18 mile of aerosol nearest the observer. The strong weighting of the aerosol near the

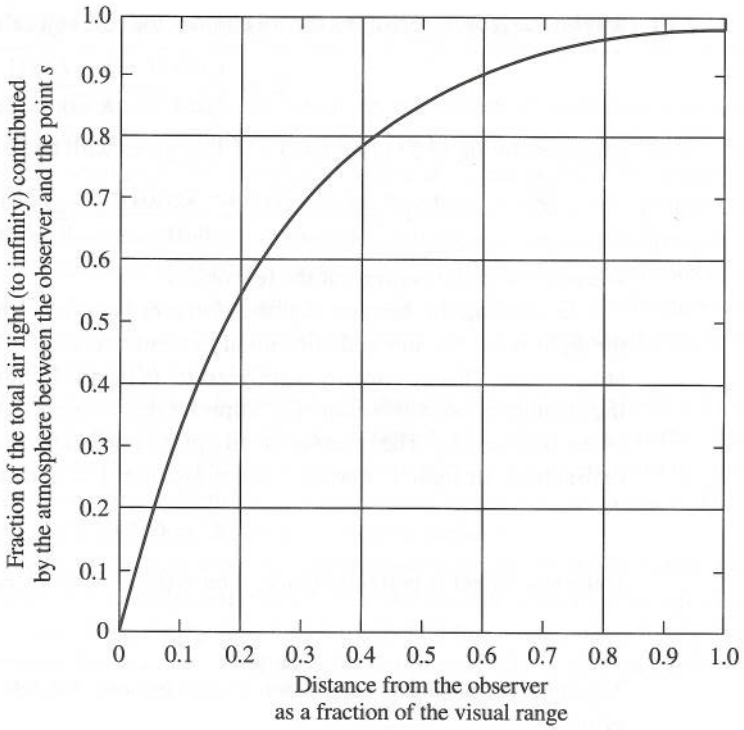

Figure 5.13 Fraction of the total air light (to infinity) contributed by the portion of the atmosphere between the observer and the point s from the observer. The air light that obscures distant objects arises mostly from the aerosol in the immediate vicinity of the observer (for a uniform atmosphere). (See Problem 6.) (After Steffens, 1956.)

observer is one reason why the idealized theoretical analysis discussed above works as well as it does. As long as the aerosol is fairly uniform in the neighborhood of the observer, the conditions beyond have little influence.

The total atmospheric extinction is the sum of contributions for the aerosol, molecular scattering, and, perhaps, some gas absorption at certain wavelengths characteristic of strong absorbers such as NO_2:

$$b = b_{\text{aerosol}} + b_{\text{molecular}} \tag{5.59}$$

Molecular scattering coefficients for air have been tabulated (Table 5.2). For $\lambda = 0.5$ μm, the visibility calculated from (5.58) is about 220 km or 130 mi. Hence the visibilities of a few miles or less, often observed in urban areas when the humidity is low, are due primarily to aerosol extinction. In some cases, however, there may be a contribution by NO_2 absorption.

TABLE 5.2
Rayleigh Scattering Coefficient for Air at 0°C and 1 atm[a] (Penndorf, 1957)

$\lambda(\mu m)$	$b_{scat} \times 10^8$ (cm^{-1})
0.2	954.2
0.25	338.2
0.3	152.5
0.35	79.29
0.4	45.40
0.45	27.89
0.5	18.10
0.55	12.26
0.6	8.604
0.65	6.217
0.7	4.605
0.75	3.484
0.8	2.684

[a]To correct for the temperature, $b_T = b_{T=0°C}(273/T\ \text{K})$ at 1 atm. This approximate formula does not take into account the variation of refractive index with temperature.

INELASTIC SCATTERING: RAMAN EFFECT

Basic Concepts

The previous discussions were limited to scattering processes in which the wavelengths of the incident and scattered light are equal (or nearly equal), that is, elastic scattering. Light may be scattered at a wavelength different from the incident beam, inelastic scattering, as a result of quantum mechanical effects. This phenomenon, known as Raman scattering, is illustrated in Fig. 5.14, which summarizes absorption and the various scattering processes discussed in this chapter. Two vibrational quantum states present in a scattering molecule are shown: the ground state $V = 0$ and the $V = 1$ energy state. The energy of the incident beam is assumed to be several times larger than the energy difference between the two states. Photons from the incident beam may raise the molecule from state 0 or 1 to a virtual state that does not correspond to any allowed state. Three outcomes are possible. The molecule may return to its original state (0 or 1) by emission of a photon with the same energy as the incident beam, equivalent to elastic scattering. Alternatively, the molecule originally in state 0 may drop to state 1 by emitting a photon of less energy than the incident beam (Stokes emission). Finally the molecule originally in state 1 may fall to state 0 by emitting a photon of higher energy than the incident beam (anti-Stokes emission). Thus the Stokes lines appear at lower frequencies and the less intense anti-Stokes lines at higher frequencies

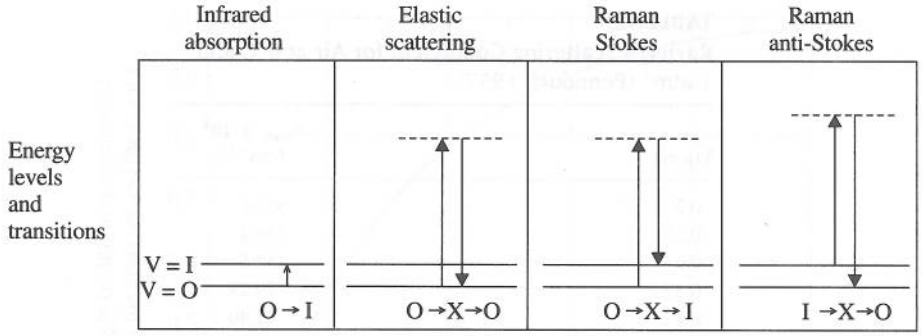

Figure 5.14 Schematic diagram illustrating infrared absorption and elastic and inelastic (Raman) scattering by a molecule with two vibrational quantum states, the ground state $\nu = 0$ and the $\nu = 1$ energy level. In infrared absorption, the incident photon has the same frequency as the molecular vibration. In elastic and inelastic scattering, the incident photon has a much higher frequency, seven times that of the vibrational quantum state in this diagram. Scattered photons are of two types: the lower ("Stokes") or higher ("anti-Stokes") frequencies ($7\nu \pm \nu$). The photon frequency difference before and after scattering is equal to the molecular vibrational frequency. (After Colthup et al., 1990, p. 61.)

than that of the incident beam. The intensity of the Raman scattering is usually several orders of magnitude smaller than that of elastic scattering.

Raman spectra have a number of features that simplify their interpretation: (1) The Raman shift or difference between the frequencies of the incident and scattered light is independent of the frequency of the incident light; (2) to a first approximation, the Raman shift is independent of the state (gas, liquid, or solid) of the scattering medium; (3) the energy corresponding to the Raman shift frequency, $h\nu_R$, is equal to the difference between the energies of two stationary states of the scattering molecules; precise information on this energy difference can be obtained from the absorption and emission spectra of the scattering material.

Raman Scattering by Particles

There are few methods suitable for on-line chemical analysis of aerosol particles. Raman spectroscopy offers the possibility of identifying the chemical species in aerosol particles because the spectrum is specific to the molecular structure of the material, especially to the vibrational and rotational modes of the molecules. Raman spectra have been obtained for individual micron-sized particles placed on surfaces, levitated optically or by an electrodynamic balance, or by monodisperse aerosols suspended in a flowing gas. A few measurements have also been made for chemically mixed and polydisperse aerosols. The Raman spectrum of a spherical particle differs from that of the bulk material because of morphology-dependent resonances that result when the Raman scattered photons undergo Mie scattering in the particle. Methods have been developed for calculating the modified spectra (McNulty et al., 1980).

Both measurements and calculations based on Raman theory indicate that the scattering intensity is approximately proportional to the particle volume (or mass) over certain

refractive index ranges and values of $\pi d_p/\lambda > 0.2$. Calculations (Fig. 5.15) show this holds best for scattering in the forward direction. Figure 5.16 shows experimental measurements of the ratio of the Raman intensity of monodisperse and polydisperse diethylsebacate aerosols to that of the nitrogen carrier gas peak as a function of aerosol mass loading for aerosols with various size distributions. Mass mean diameters ranged from 0.4 to 1.8 μm, and the mass loadings ranged from 0.4 to 13 g/m^3. The figure shows that the Raman signal is approximately independent of the size distribution over this range and is proportional to the total mass concentration. Neither the theoretical calculations nor the experimental measurements show a strong effect of the morphology-dependent resonances on the relationship of the scattering intensity to particle volume for spherical particles.

The mass loadings in these studies were high, with the lowest approximately 0.4 g/m^3. These concentrations fall in the range of some industrial and therapeutic aerosols but are several orders of magnitude higher than atmospheric aerosol concentrations. Buehler et al. (1991) also found an approximate dependence of scattering on particle volume for large suspended single droplets ($25 < d_p < 66$ μm). These results suggest that at sufficiently high mass loadings it may be possible to monitor the mass concentration of Raman active

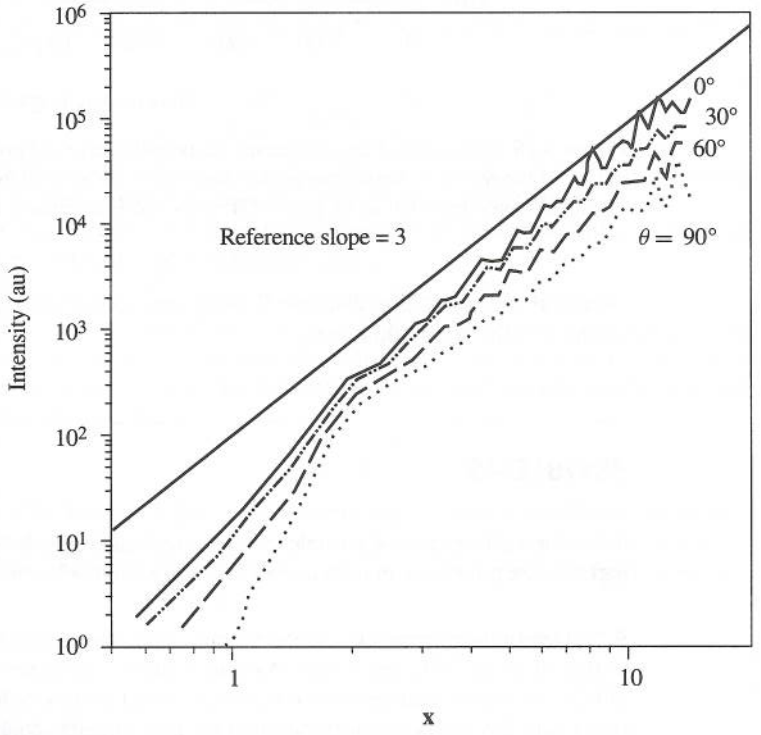

Figure 5.15 Calculated values of the intensity of Raman scattering at various values of the scattering angle for $m = 1.5$. The intensity is approximately proportional to the particle volume for $x > 2$ (Stowers and Friedlander, 1998).

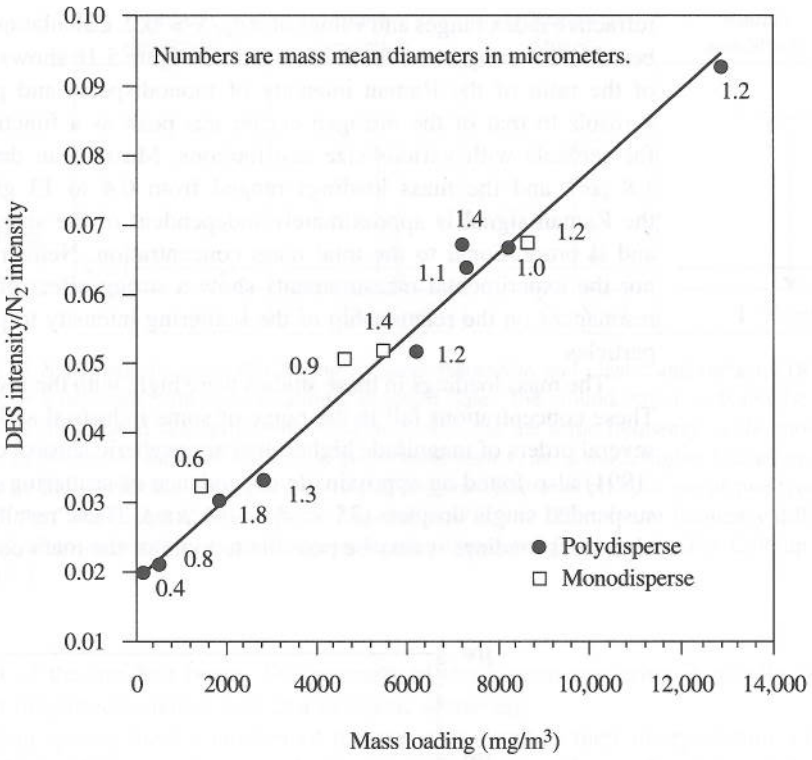

Figure 5.16 Ratio of the Raman intensity of monodisperse and polydisperse diethylsebacate aerosols to that of the nitrogen carrier gas peak. Mass mean diameters ranged from 0.4 to 1.8 μm, and mass loadings ranged from 0.4 to 13 g/m^{-3} (Stowers and Friedlander, 1998).

chemical species in polydisperse flowing aerosols composed of particles larger than a few tenths of a micron in diameter.

PROBLEMS

5.1 For a given mass of particles with the optical properties of carbon spheres, determine the particle size producing maximum extinction for $\lambda = 0.436$ μm. Assume monodisperse particles.

5.2 Determine the particle concentration (μg/m^3) necessary to scatter an amount of light equal to that of air at 20°C and 1 atm. Assume a particle refractive index of 1.5 and a wavelength of 0.5 μm. Do the calculation for 0.1-, 0.5-, and 1-μm particles of unit density. Compare your result with the average concentration in the Los Angeles atmosphere, about 100 μg/m^3.

5.3 The California visibility standard requires that the visibility be greater than 10 miles on days when the relative humidity is less than 70%. Consider a day when the visibility controlling

aerosol is composed of material with a refractive index of 1.5. Estimate the aerosol concentration in the atmosphere that would correspond to the visibility standard. Assume (1) the density of the spherical particles is 1 g/cm^3; (2) the aerosol is monodisperse with a particle size, $d_p = 0.5$ μm; and (3) the wavelength of interest is 0.5 μm. Express your answer in micrograms of aerosol per cubic meter of air.

5.4 The extinction of light by an aerosol composed of spherical particles depends on its optical properties and size distribution. Consider the distribution function $n_d(d_p) \sim d_p^{-4}$, often observed at least approximately. Suppose these particles are composed of an organic liquid ($m = 1.5$), on the one hand, or of carbon, on the other. This might correspond to a photochemical aerosol ($m = 1.5$) and a soot aerosol generated by a diesel source or other combustion processes. Calculate the ratio $b_{\text{carbon}}/b_{1.5}$ for fixed size distribution.

5.5 It is possible, in principle, to determine the size distribution of particles of known optical properties by measurement of the light scattered by a settling aerosol. In this method, the intensity of the light transmitted by the aerosol in a small cell, I, is recorded as a function of time. The aerosol is initially uniform spatially, and there is no convection.

The light scattered from a horizontal beam at a given level in the cell remains constant until the largest particles in the aerosol have had time to fall from the top of the cell through the beam. The scattering will then decrease as successively smaller particles are removed from the path of the beam.

Show that the size distribution function can be found from the relationship (Gumprecht and Sliepcevich, 1953)

$$-\frac{1}{I}\frac{dI}{dt} = LQ_{\text{sca}}\frac{\pi d_p^{*2}}{4}n_d\left(d_p^*\right)\frac{d\left(d_p^*\right)}{dt}$$

where d_p^* is the maximum particle size in the beam at any time, t, and L is the length of the light path (cell thickness). Describe how d_p^* and $d(d_p^*)/dt$ can be determined.

In practice, the system will tend to be disturbed by Brownian diffusion and convection, and this method is seldom used to determine $n_d(d_p)$.

5.6 Let J be the intensity of the air light seen by an observer looking along a horizontal path to the horizon sky (infinity). The path falls close to one that ends at a black test object a distance s from the observer. (a) Show that the intensity of the light seen by an observer looking toward the black test object is given by

$$I(s) = J\left(1 - e^{-bs}\right)$$

where s is the distance of the observer from the test object. (b) Derive an expression for the fraction of the total air light (to infinity) contributed by the atmosphere between the observer and the point s from the observer. This is the expression on which Fig. 5.13 is based (Steffens, 1956).

REFERENCES

Barber, P. W., and Hill, S. C. (1990) *Light Scattering by Particles: Computational Methods*, World Scientific, Singapore.

Bayvel, L. P., and Jones, A. R. (1981) *Electromagnetic Scattering and Its Applications*, Applied Science Publishers, Essex, England.

Berne, B. J., and Pecora, R. (1976) *Dynamic Light Scattering*, Wiley-Interscience, New York.

Bohren, C. F., and Huffman, D. R. (1983) *Absorption and Scattering of Light by Small Particles*, Wiley, New York.

Bolz, R. E., and Tuve, G. E. (Eds.) (1970) *Handbook of Tables for Applied Engineering Science*, Chemical Rubber Company, Cleveland, OH, p. 159.

Buehler, M. F., Allen, T., and Davis, E. J. (1991) *J. Colloid Interface Sci.*, **146,** 79.

Chandrasekhar, S. (1960) *Radiative Transfer,* Dover, New York. This is the classic reference on the equation of radiative transfer and its solutions.

Colthup, N. B., Daly, L. H., and Wibberly, S. E. (1990) *Introduction to Infrared and Raman Spectroscopy*, 3rd ed., Academic Press, San Diego.

Dahneke, B. E. (1983) (Ed.) *Measurement of Suspended Particles by Quasi-Elastic Light Scattering*, Wiley-Interscience, New York.

Ensor, D. S., Charlson, R. J., Ahlquist, N. C., Whitby, K. T., Husar, R. B., and Liu, B. Y. H. (1972) *J. Colloid Interface Sci.,* **39,** 242; also in Hidy, G. M. (Ed.) (1972) *Aerosols and Atmospheric Chemistry,* Academic, New York.

Garvey, D. M., and Pinnick, R. G. (1983) *Aerosol Sci. Technol.*, **2**, 477.

Goody, R. M. (1964) *Atmospheric Radiation: I. Theoretical Basis,* Oxford University Press, Oxford. This monograph includes application of the theory of small particle scattering and the equation of radiative transfer to Earth's atmosphere.

Graham, S. C., and Homer, J. B. (1973) *Faraday Symp.*, **7**, 85.

Gumprecht, R. D., and Sliepcevich, C. M. (1953) *J. Phys. Chem.,* **57,** 95.

Hodkinson, J. R. (1966) The Optical Measurement of Aerosols, in Davies, C. N. (Ed.), *Aerosol Science,* Academic, New York.

Kerker, M. (1969) *The Scattering of Light and Other Electromagnetic Radiation*, Academic, New York. This includes a very good discussion of Mie theory with helpful physical insights as well as references to related experimental studies.

McCartney, E. J. (1976) *Optics of the Atmosphere*, Wiley, New York.

McDonald, J. E. (1962) *J. Appl. Meteor.*, **1**, 391.

McNulty, P. J., Chew, H. W., and Kerker, M. (1980) in Marlow, W. W. (Ed.) *Aerosol Microphysics I: Particle Interaction*, Springer, p. 89.

Middleton, W. E. K. (1952) *Vision Through the Atmosphere*, University of Toronto Press.

Penndorf, R. B. (1957) *J. Opt. Soc. Am.*, **47**, 176.

Steffens, C. (1956) Visibility and Air Pollution, in Magill, P. L., Holden, F. R., and Ackley, C. (Eds.), *Air Pollution Handbook*, McGraw-Hill, New York.

Stowers, M. A., and Friedlander, S. K. (1998) Paper presented at the AIChE Meeting in Miami, November 15–20.

van de Hulst, H. C. (1957) *Light Scattering by Small Particles*, Wiley, New York. This is a good place to turn for detailed information on elastic light scattering by single elements, including spheres and other bodies of simple shapes. It is primarily a theoretical work but includes several chapters on practical applications.